

Raman Spectroscopic Investigation of H₂, HD, and D₂ Physisorption on Ropes of Single-Walled, Carbon Nanotubes

Keith A. Williams, Bhabendra K. Pradhan, and Peter C. Eklund*

Milen K. Kostov and Milton W. Cole

*Physics Department, The Pennsylvania State University,
104 Davey Laboratory, University Park, PA 16802*

(November 2, 2018)

We have observed the S- and Q-branch Raman spectra of H₂, HD, and D₂ adsorbed at 85 K and pressures up to 8 atm on single-walled, carbon nanotubes (SWNT). Comparative data for H₂ on graphite and C₆₀ were also collected. For each adsorbate, we observed a small shift in the Q-branch frequencies relative to the gas-phase values. To aid in interpreting this result, we constructed an H₂-surface potential, including van der Waals and electrostatic terms. Computed shifts based on this potential are in good agreement with our data.

Single-walled, carbon nanotubes (SWNT) are nanoporous, all-surface macromolecules which may be ideal storage media for H₂ [1,2]. In addition, H₂ has been predicted to exhibit novel, quasi-1D phases in SWNT ropes [3,4]. Desorption experiments suggest the presence of a high-energy binding site for H₂ in purified and sonicated SWNT material, which has been proposed to be indicative of charge transfer [5,6]. On the other hand, transport data for SWNT suggest that H₂ physisorbs [7]. An improved understanding of the adsorption of H₂ on SWNT is the motivation for the work described here. We have collected the S- and Q-branch Raman spectra of H₂, HD, and D₂ adsorbed on SWNT at 85 K and at pressures up to 8 atm. The magnitude of the shifts in the Q-branch frequencies of these species when adsorbed on SWNT is a measure of the strength of the adsorption potential. For physisorption, the shifts should be small, while in the event of charge transfer, the shifts should be large: the change of the H₂ stretching frequency with the molecular charge is $\sim 2000 \text{ cm}^{-1}$ per electron [15]. The approach taken in this work is similar to that described in Ref. [8], except that we have employed Raman rather than IR spectroscopy.

Using a two-step, oxidative and acid reflux technique, we obtained SWNT samples containing minimal amorphous and multishell carbon (<15 wt-%) and residual metal catalyst (<10 wt-%, <2 atom-%), as determined by temperature programmed oxidation. This material was annealed in a vacuum of better than 10^{-7} Torr at 1200 K for 24 hours; such high-temperature “degassing” was recently shown to remove the carboxylic and related functional groups occluding the SWNT ends and side walls [10]. The resulting material was pressed against indium foil and inserted in an optical pressure cell, which was placed in a cryostat (Janis Corp. Model VPF 700, 77-700 K) with a gas line to the cell. The cell was valved to a diffusion pump and to the cylinders of H₂ (ultra-high purity, 99.999%, MG Industries), HD (97.4 mol-%, with 1.4% H₂ and 1.2% D₂, Isotec Inc.), and D₂ (ultra-high purity, 99.999%, MG Industries). In separate experiments, samples of C₆₀ powder (Alfa Aesar, 99.9%, packed under Ar) and freshly cleaved, pyrolytic graphite (Alfa Aesar) were loaded into our cell.

Raman spectra were collected in the backscattering geometry, with $\lambda_{air}=514.53 \text{ nm}$ excitation provided by a mixed-gas, Ar/Kr-ion laser (Coherent Inc., Innova Spectrum). The incident beam was focused through the windows of the cryostat and pressure cell onto the sample surface. Backscattered Rayleigh light was rejected by a holographic “super-notch” filter (Kaiser, Inc.), and Raman light was focused through a $25 \mu\text{m}$ slit into a single-grating monochromator (Instruments S.A. HR460, grating: 1800 grooves/mm) equipped with a CCD. To correct our spectra for slight, instrumental nonlinearity and to calibrate the spectra, one Hg line and several pairs of Ne lines close to the Q-branch lines of H₂, D₂, and HD were used. The Ar, Hg and Ne frequencies were taken from Refs. [16] and [17].

For all data reported here, the sample temperature was $85 \pm 5 \text{ K}$, and the pressure of the adsorbate gas on the sample was increased from vacuum to as high as 8 atm, in the case of H₂ and D₂, and to 5 atm in the case of HD. Typical S- and Q-branch spectra at 8 atm are shown in Figs.1 and 2; we use the notation $S(J)$ or $Q(J)$ to denote transitions, in which J is the initial state. The frequencies, ν_{ads} , of the observed S- and Q-branch transitions are given in Table 1; these values were determined by fitting Voigt-profile functions to the spectra using Humlíček’s algorithm [12]. Also provided in Table-1 are the frequencies, ν_{free} , of these transitions for free molecules, from Ref. [15].

Our S-branch data suggest freely rotating molecules in the gas phase, and are in good agreement with recent inelastic neutron scattering data [18]. Small, downshifted shoulders are evident in the S-branch lines, but our experimental

*To whom correspondence should be addressed; email: pce3@psu.edu

resolution is insufficient to quantify these effects. Our Q-branch data for HD and D₂ contain prominent bands which are slightly upshifted from the free-molecule frequencies (see Table 1), but, due to the small splitting of the J=0 and J=1 bands, the peak substructure could not be resolved. Our data for H₂ in SWNT are considerably more illuminating, and are shown in expanded form in Fig.3 at two pressures, along with comparative data for C₆₀ and highly-oriented pyrolytic graphite (HOPG) collected at 85±5 K and 4 atm. The best fits (solid curves) to the data in Fig.3 were computed using a sum of Voigt components (dashed curves).

The surface area of HOPG is extremely small, so the signal strength from adsorbed molecules should be negligible. Therefore, we assign the bands observed at 4161.3 and 4155.4 cm⁻¹ to gas-phase H₂ near the surface; these frequencies are in reasonable agreement with the those reported by May, *et al* [13]. The gas-phase components should also be present in the data on C₆₀ and SWNT, and so our analysis of these data proceeded by inserting components of frequency and width equal to those observed on HOPG, and then introducing separate Voigt components to describe the additional bands. Consistent with this approach, we noted an approximately twofold increase in the relative intensities of the bands attributed to gas-phase species, as the pressure was increased from 4 to 8 atm. In our analysis of the data on SWNT at 8 atm, the positions of the bands attributed to the gas phase were allowed to vary, and the frequencies were found to be ~0.1 cm⁻¹ lower, again consistent with the data of May, *et al* [13].

In addition to the gas-phase components, it is clear that the data for C₆₀ and SWNT contain additional bands which are lacking in the data on HOPG. We ascribe these components to adsorption in the interstices or internal pores in the respective lattices. Neutron powder diffraction work by FitzGerald, *et al.*, has indicated the existence of an adsorbed phase in the octahedral sites of *fcc*-C₆₀ [11]; presumably, these sites are partially filled under the conditions of our study and account for the lower-frequency component present in our Q-branch data for H₂ on C₆₀.

A reduction in the number of fitting parameters was achieved by setting equal the linewidth parameters of equally-spaced pairs of Q(0) and Q(1) peaks. All parameters were then refined until χ^2 was minimized and the frequencies were obtained. Our confidence in the number of Voigt components introduced for each data set is affirmed by the relative intensities between “pairs” of Voigt components: $I_{Q(1)}/I_{Q(0)}=2.2-2.5$, in good agreement with the equilibrium ortho-para ratio at 85 K. Also, the Q(1)-Q(0) spacing we find between these pairs (5.8–6.0 cm⁻¹) is consistent with the value (~5.97 cm⁻¹) reported by May, *et al*, under similar conditions [13].

Based on shifts observed in the tangential Raman bands of SWNT material previously dosed with H₂, partial electron transfer from SWNT to the H₂ adsorbate has been proposed [6]. Our experiment is uniquely suited to looking for such effects, given the extreme sensitivity of the H₂ stretching frequency on the molecular charge state. Contrary to reports on certain zeolites and oxides [8], no strongly shifted Q-branch lines were observed on SWNT. This would seem to rule out significant charge transfer under our experimental conditions.

To aid in interpreting the small shifts found in our Q-branch data, we have constructed an interaction potential for H₂ with graphene (a single sheet of graphite) and estimated the frequency shifts in two types of adsorption sites. For the case of H₂ adsorbed on graphene, the potential is a sum of C-H van der Waals interactions, U_{LJ} , and the electrostatic interaction, U_{el} , of the H₂ static multipole moments with the static screening charges induced on the graphene surface [19]. Because the low-frequency dielectric response of graphene is metallic [20], the screening charges may be represented by full image charges displaced from the graphene sheet by a distance z_0 . The electrostatic interaction can be expressed in terms of the H₂ quadrupole (Θ) and hexadecapole (Φ) moments [19]:

$$\Phi_{el}(z_0, \theta) = -\frac{3k\Theta^2}{8(2z_I)^5}[3\cos^4\theta + 2\cos^2\theta + 3] - \frac{15k\Theta\Phi}{16(2z_I)^7}[7\cos^6\theta + 5\cos^4\theta + 9\cos^2\theta - 5], \quad (1)$$

where z_c is the perpendicular distance from the molecular center to the surface atoms, $z_I = z_c - z_0$ is the location of the image with respect to the graphene surface, θ is the angle of the molecular axis with respect to the surface normal, and k is the usual electrostatic constant. In view of the small surface corrugation, the holding potential is $V(z_c, \cos\theta) = U_{el} + U_{LJ}(z_1) + U_{LJ}(z_2)$, where the z_i are the perpendicular distances of the H atoms relative to the surface, and the $U_{LJ}(z_i)$ are the corresponding, pairwise van der Waals interactions. The C – H interactions are assumed to be of Lennard-Jones (12-6) form, and for simplicity, we smear out the C atoms along the surface. In this approximation,

$$U_{LJ}(z) = 2\pi\vartheta\epsilon_{C-H}\sigma_{C-H}^2\left[\frac{2}{5}\left(\frac{\sigma_{C-H}}{z}\right)^{10} - \left(\frac{\sigma_{C-H}}{z}\right)^4\right], \quad (2)$$

where $\vartheta = 0.38 \text{ \AA}^{-2}$ is the surface density of the C atoms. We adopted the values $\epsilon_{C-H} = 2.26 \text{ meV}$, $\sigma_{C-H} = 2.76 \text{ \AA}$ [21].

The least well-known parameter in our potential is z_0 [22]. To obtain this parameter, we computed the minimum of the C-H₂ potential at the equilibrium distance z_{eq} , where H₂ is preferentially oriented flat against the surface. In the case of a graphene sheet, the isotropic C-H₂ holding potential has the same functional form as Eqn.(2), with a minimum at $z_{eq} = \sigma_{C-H_2}$. Using $\epsilon_{C-H_2} = 42.8 \text{ K}$ and $\sigma_{C-H_2} = 2.97 \text{ \AA}$ [24], the resulting well depth is 46.6 meV.

The values for the H₂ moments, taken from Ref. [25], are $\Theta = 0.48917$ a.u.; $\Phi = 0.230063$ a.u.. These values yield $z_0 = 1.36$ Å, a value consistent with previous *ab initio* and empirical estimates for this system [23].

For the study of H₂ in the ICs, we adapted a potential, U_{LJ}^* , already developed for a single nanotube [26]. The dispersion part of this potential ignores many-body effects, considers the C atoms to be smeared on the surface, and is isotropic. When averaged over the azimuthal and longitudinal coordinates, this potential takes the form [26]:

$$U_{LJ}^*(z) = 3\pi\theta\epsilon_{C-H}\sigma_{C-H}^2 \left[\frac{21}{32} \left(\frac{\sigma_{C-H}}{R} \right)^{10} f_{11}(x)M_{11}(x) - \left(\frac{\sigma_{C-H}}{R} \right)^4 f_5(x)M_5(x) \right], \quad (3)$$

in which z is the distance from the axis of a nanotube with nuclear radius R ; we define $x = R/z$ and $f_l(x) = (R/z)^l$, with the l being positive integers. The M_l are integrals defined in Ref. [26]. The potential for an IC is obtained by summing U_{LJ}^* over an assembly of three nanotubes and azimuthally averaging the result.

The electrostatic portion of the potential in the ICs contains two contributions, denoted U_1 and U_2 , which arise, respectively, from the interaction of the H₂ quadrupole moment with the local electrostatic field of the SWNT, and the interaction of the H₂ static multipole moments with the screening charges induced on the surface. U_1 is given by

$$U_1(z_c, \cos\theta) = -\frac{1}{6} \sum_{i,j} \Theta_{ij} \frac{\partial^2 \Phi(z_c)}{\partial x_i \partial x_j}, \quad (4)$$

in which the Θ_{ij} are the components of the quadrupole moment and Φ is the local electrostatic field, which was calculated from first principles for “zigzag” SWNT with radius $R = 6.9$ Å [27]. To evaluate U_2 , we included the H₂ quadrupole moment (which is the first nonzero permanent moment of an axial quadrupole), and the hexadecapole moment. This problem is quite complicated, so we introduce three simplifications. Due to the small size of the H₂ molecule, we consider its multipoles to be “point”-like. Next, to simplify the complex geometry of the IC, we represent the SWNT walls with graphene planes. The locations of the image charges are determined by the boundary condition requiring that the potential be zero at each plane. Finally, we assumed that the graphene planes are perfectly conducting, so that the static and dynamic responses are represented by images. We adopted the same value for z_0 and the same form for the interaction as in the previous case.

To compute the vibrational frequency shift, the total holding potential U must be expressed as a function of the relative bondlength change, $\xi = (r - r_e)/r_e$, relative to the equilibrium value, r_e , and also of the configuration τ of the molecule. Given a sufficiently small H₂-substrate interaction, one can treat U and the anharmonic terms in the potential energy function of the free H₂ molecule as perturbations to the harmonic oscillator Hamiltonian [9]. Using first- and second-order perturbation theory, the change in the frequency of the fundamental ($n=0 \rightarrow n=1$) transition due to U is [9,28]:

$$\Delta\omega = \Delta\omega_{1\leftarrow 0} = \frac{B_e}{\hbar\omega_e} \langle U'' - 3aU' \rangle_{\tau} + O\left(\frac{B_e}{\hbar\omega_e}\right)^2. \quad (5)$$

in which B_e is the equilibrium rotational constant, a is the anharmonicity, primes denote derivatives with respect to ξ , and the angled brackets denote the average over all τ . The expressions for $\Theta(r)$ and $\Phi(r)$ were derived via a model in which the electron cloud is concentrated between the nuclei rather than about each individual nucleus. Assuming an H₂ bondlength of 0.71 Å, and placing the electrons symmetrically on the molecular axis, separated by 0.48 Å, the experimental value of the H₂ quadrupole moment is reproduced. From this model, we find $\Theta \sim r^2$ and $\Phi \sim r^4$, for small changes in ξ about r_e .

Regarding the orientational dependence, U' and U'' are functions of the z -displacement of molecular center-of-mass, and of the polar (θ) and azimuthal (ϕ) angles. U depends on z_c , so the translational and rotational parts of $U'(z_c; \theta, \phi)$, $U''(z_c; \theta, \phi)$ do not decouple exactly. To separate the variables, we treat the interaction of translational and rotational modes in a mean-field manner [29]. The effective interaction was computed by averaging the derivatives of Eqn.5 over the center-of-mass vibrations of the molecule. Treating these as modes of a simple harmonic oscillator, the *rms* deviations in the z -position are found to be $\delta z_{rms} = 0.298$ Å on a single graphene surface, and $\delta z_{rms} = 0.225$ Å for H₂ in an IC. Next, to compute $\langle U' \rangle_{\tau}$ and $\langle U'' \rangle_{\tau}$, variations were performed with respect to r in the adsorption potential for different τ . Finally, we averaged over all orientations (θ, ϕ) of the molecular axis.

Using the values $a=-1.6$ and $B_e/\hbar\omega_e=0.0138$ [28], we find that for the case of H₂ adsorbed on graphene, our procedure predicts an upshift of $\Delta\omega_{1\leftarrow 0}=1.4$ cm⁻¹ ($\langle 3aU' \rangle = -126.2$ cm⁻¹, $\langle U'' \rangle = -28.3$ cm⁻¹). In contrast, for H₂ adsorbed in an IC, we predict a *downshift* of $\Delta\omega_{1\leftarrow 0}=-2.9$ cm⁻¹ ($\langle 3aU' \rangle = 168.0$ cm⁻¹, $\langle U'' \rangle = -42.2$ cm⁻¹). We expect similar results for D₂: the same potential parameters and quadrupole moment may be assumed, though a and $B_e/\hbar\omega_e$ are smaller [14], and should lead to smaller shifts. In the case of HD, the center of mass and charge do not coincide, leading to a larger Lennard-Jones contribution to the potential and a larger upshift.

In summary, we have observed several lines within the rotational and vibrational Raman spectra of H₂, HD, and D₂ adsorbed on SWNT; observed frequency shifts are small and consistent with physisorption. Comparative Q-branch data for H₂ on C₆₀ reveal substructure in the Q-branch, which appears to arise from H₂ adsorbed in different sites. An interaction potential was developed to estimate the frequency shifts of the adsorbate vibrational modes; our results support the multiple-site interpretation of our data. We wish to thank Vin Crespi, Roger Herman, John Lewis, and Dragan Stojkovic for their generous contributions to this work. This work was funded by the Department of Energy and the Army Research Office. PCE and KAW were funded, in part, by the Office of Naval Research.

- [1] M.S. Dresselhaus, K.A. Williams, and P.C. Eklund, *MRS Bulletin* **24**(11),(1999), 45-50.
- [2] K.A. Williams, and P.C. Eklund, *Chem. Phys. Lett.* **320**(2000), 352-358.
- [3] M.M. Calbi, S.M. Gatica, M.J. Bojan, G. Stan and M.W. Cole, submitted to *Rev. Mod. Phys.*; <http://xxx.lanl.gov/abs/cond-mat/0103607>.
- [4] M.W. Cole, V.H. Crespi, G. Stan, J.M. Hartman, S. Moroni, and M. Boninsegni, *Phys. Rev. Lett.* **84**, 3887 (2000).
- [5] A.C. Dillon, and M.J. Heben, *Applied Physics A* **72**(2001), 133-142.
- [6] M.J. Heben, A.C. Dillon, T. Gennett, J.L. Alleman, P.A. Parilla, K.M. Jones, and G.L. Hornyak, *Proc. Mat. Res. Soc.*, in press.
- [7] C.K.W. Adu, G.U. Sumanasekera, B.K. Pradhan, H.E. Romero, and P.C. Eklund, *Chem. Phys. Lett.* **337** 31–35 (2001).
- [8] W.C. Conner, in *Physical Adsorption: Experiment, Theory, and Applications*, F. Fraissard (ed.), NATO ASI Series C **491**.
- [9] A.D. Buckingham, *Proc. Roy. Soc. A* **248**, 169 (1959).
- [10] A. Kuznetsova, D.B. Macwhinney, V. Naumenko, J.T. Yates Jr., J. Liu, and R.E. Smalley, *Chem. Phys. Lett.* **321**(2000), 292–296.
- [11] S.A. Fitzgerald, T. Yildirim, L.J. Santodonato, D.A. Neumann, J.R.D. Copley, and J.J. Rush, *Phys. Rev. B* **60**(9) 6439–6451 (1999).
- [12] J. Humlíček, *Journal of Quantitative Spectroscopy and Radiative Transfer*, **27**(4) 437–444 (1982).
- [13] A.D. May, G. Varghese, J.C. Stryland, and H.L. Welsh, *Can. J. Phys.* **42**(1964), 1058–1069.
- [14] G. Herzberg, *Molecular Spectra and Molecular Structure: I. Spectra of Diatomic Molecules*, (Van Nostrand Reinhold, New York, 1950).
- [15] K.P. Huber, G. Herzberg, *Molecular Spectra and Molecular Structure: IV. Constants of Diatomic Molecules*, (Van Nostrand Reinhold, New York, 1979).
- [16] G. Norlén, *Physica Scripta* **8** 249–268 (1973).
- [17] K. Burns, K.B. Adams, and J. Longwell, *J. Opt. Soc. Am.* **40**(6) 339–344 (1950).
- [18] C.M. Brown, T. Yildirim, D.A. Neumann, M.J. Heben, T. Gennett, A.C. Dillon, J.L. Alleman, and J.E. Fischer, *Chem. Phys. Lett.* **329** (2000) 311–316.
- [19] L.W. Bruch, *Surf. Sci.* **125**, 194 (1983).
- [20] H.R. Philipp, *Phys. Rev. B* **16**, 2896 (1977).
- [21] W.B.J.M. Janssen, T.H.M. van den Berg, and A. van der Avoird, *Phys.Rev. B* **43**, 5329 (1991).
- [22] F.Y. Hansen, L.W. Bruch, and S.E. Roosevelt, *Phys.Rev. B* **45**, 11238 (1992).
- [23] H.Y. Kim, and M.W. Cole, *Phys.Rev. B* **35**, 3990 (1987).
- [24] S.C. Wang, L. Senbetu, and C.W. Woo, *J. Low Temp. Phys.* **41**, 611 (1980).
- [25] G. Maroulis and D.M. Bishop, *Chem.Phys.Lett.* **128**, 462 (1986).
- [26] G. Stan and M.W. Cole, *Surf. Sci.* **395**, 280 (1998).
- [27] These calculations were performed using the PARATEC package developed at U.C. Berkeley.
- [28] R.M. Herman and S. Short, *J. Chem. Phys.* **48**, 1266 (1968).
- [29] A.D. Novaco and J.P. Wroblewski, *Phys. Rev. B* **39**, 11364 (1989).

Adsorbate species	Transition	ν_{free} (cm^{-1})	ν_{ads} (cm^{-1})	$\Delta\nu$ (cm^{-1})
H ₂	Q(0)	4160.5	4162.3	+1.8
			4161.1	+0.6
			4159.3	-1.2
	Q(1)	4154.4	4156.4	+2.0
			4155.2	+0.8
			4153.5	-0.9
	S(0)	354.4	354.8	+0.4
S(1)	587.0	587.5	+0.5	
HD	Q(0)	3629.8	3632.5	+2.7
	Q(1)	3625.8	3628.8	+0.6
	Q(2)	3620.5	3620.9	+0.4
	S(0)	267.1	267.7	+0.6
	S(1)	443.1	444.1	+1.0
D ₂	Q(0)	2993.5	2993.8	+0.3
	Q(1)	2991.4	2991.9	+0.5
	Q(2)	2987.2	2987.5	+0.3
	S(0)	179.1	178.5	-0.6
	S(1)	297.5	297.8	+0.3

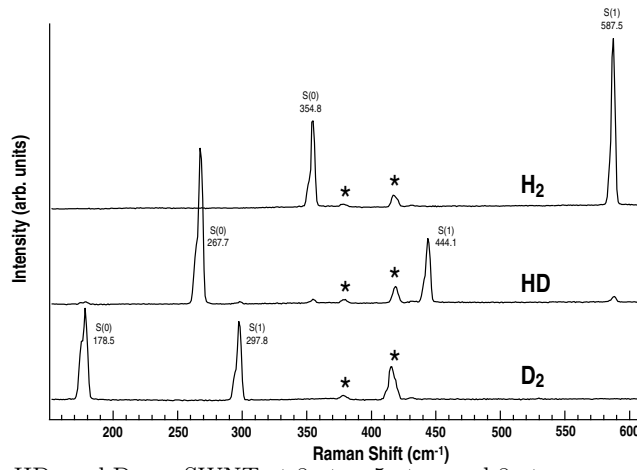


FIG. 1. S-branch data for H₂, HD, and D₂ on SWNT at 8 atm, 5 atm, and 8 atm, respectively. Asterisks indicate unrelated lines due to external calibration sources.

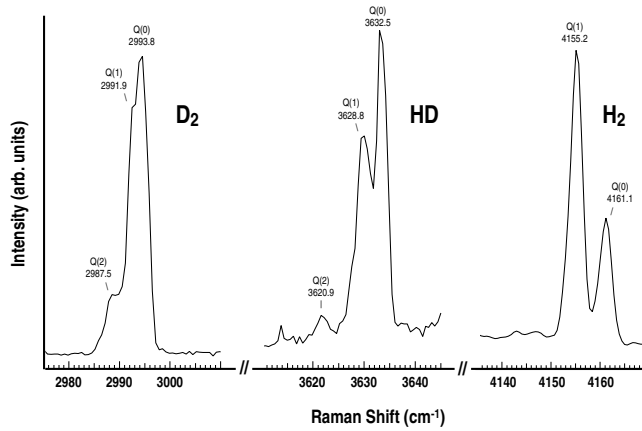


FIG. 2. Q-branch data for H₂, HD, and D₂ on SWNT at 8 atm, 5 atm, and 8 atm, respectively. For comparisons of these peak positions with the frequencies of the free molecules, see Table 1.

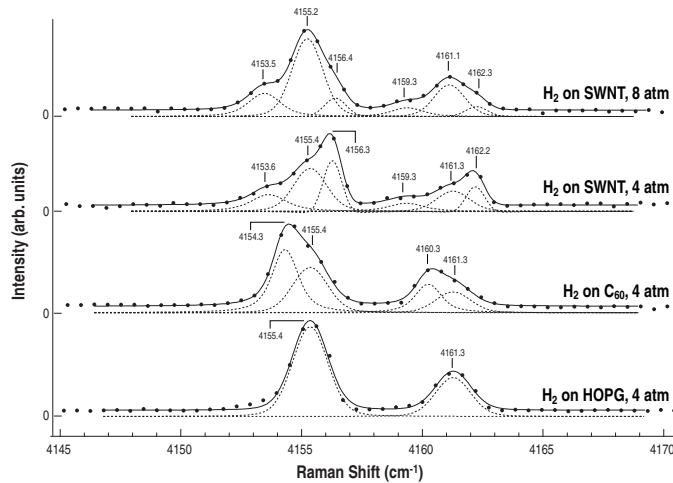


FIG. 3. Q-branch data for H₂ on SWNT at 8 and 4 atm, together with data for C₆₀ and HOPG at 4 atm.